

High temperature reactive ion etching of iridium thin films with aluminum mask in $\text{CF}_4/\text{O}_2/\text{Ar}$ plasma

Chia-Pin Yeh, Marco Lisker, Bodo Kalkofen, and Edmund P. Bulte

Citation: *AIP Advances* **6**, 085111 (2016); doi: 10.1063/1.4961447

View online: <https://doi.org/10.1063/1.4961447>

View Table of Contents: <http://aip.scitation.org/toc/adv/6/8>

Published by the [American Institute of Physics](#)

Articles you may be interested in

[Etch characteristics of iridium in chlorine-containing and fluorine-containing gas plasmas](#)

Journal of Vacuum Science & Technology A: Vacuum, Surfaces, and Films **19**, 2400 (2001); 10.1116/1.1385912

[Effect of temperature on etch rate of iridium and platinum in \$\text{CF}_4/\text{O}_2\$](#)

Journal of Vacuum Science & Technology A: Vacuum, Surfaces, and Films **19**, 1312 (2001); 10.1116/1.1353541

[Overview of atomic layer etching in the semiconductor industry](#)

Journal of Vacuum Science & Technology A: Vacuum, Surfaces, and Films **33**, 020802 (2015); 10.1116/1.4913379

[Plasma etching of Si and \$\text{SiO}_2\$ in \$\text{SF}_6\text{-O}_2\$ mixtures](#)

Journal of Applied Physics **52**, 162 (1981); 10.1063/1.328468

[Plasma etching: Yesterday, today, and tomorrow](#)

Journal of Vacuum Science & Technology A: Vacuum, Surfaces, and Films **31**, 050825 (2013); 10.1116/1.4819316

[Low-temperature reactive ion etching and microwave plasma etching of silicon](#)

Applied Physics Letters **52**, 616 (1988); 10.1063/1.99382

PHYSICS TODAY

WHITEPAPERS

MANAGER'S GUIDE

Accelerate R&D with
Multiphysics Simulation

READ NOW

PRESENTED BY

 COMSOL

High temperature reactive ion etching of iridium thin films with aluminum mask in $\text{CF}_4/\text{O}_2/\text{Ar}$ plasma

Chia-Pin Yeh,¹ Marco Lisker,² Bodo Kalkofen,^{1,a} and Edmund P. Bulte¹

¹*Institute of Micro and Sensor Systems, Otto von Guericke University Magdeburg, Universitätsplatz 2, 39106, Magdeburg, Germany*

²*IHP, Im Technologiepark 25, 15236 Frankfurt (Oder), Germany*

(Received 20 June 2016; accepted 4 August 2016; published online 16 August 2016)

Reactive ion etching (RIE) technology for iridium with $\text{CF}_4/\text{O}_2/\text{Ar}$ gas mixtures and aluminum mask at high temperatures up to 350 °C was developed. The influence of various process parameters such as gas mixing ratio and substrate temperature on the etch rate was studied in order to find optimal process conditions. The surface of the samples after etching was found to be clean under SEM inspection. It was also shown that the etch rate of iridium could be enhanced at higher process temperature and, at the same time, very high etching selectivity between aluminum etching mask and iridium could be achieved. © 2016 Author(s). All article content, except where otherwise noted, is licensed under a Creative Commons Attribution (CC BY) license (<http://creativecommons.org/licenses/by/4.0/>). [<http://dx.doi.org/10.1063/1.4961447>]

I. INTRODUCTION

Reactive ion etching (RIE)/plasma etching is widely used in modern IC technology to form device structures, connections between devices, and various patterns, which are defined by photolithography. However, many difficulties exist when applying this method to the formation of ferroelectric capacitors with iridium (Ir) electrodes for the application of ferroelectric random access memories (FeRAMs). Halogen-containing gases are often used in reactive ion etching processes to form volatile compounds of etched materials and these volatile compounds are pumped away from the substrates thereafter. Unfortunately, halogen-containing gases form low volatile compounds with the electrode material Ir. Table I shows the melting and boiling points of most of the halides of Ir. They have high melting and boiling points, are therefore nonvolatile at room temperature.

In comparison to plasma etching of silicon with CF_4 , the etching product SiF_4 has a melting point at -90.2 °C and a boiling point at -86 °C. Low volatility of the etching products means difficulty to remove the etching products from the etched surface and hence low etching rates. It is apparent that iridium is more difficult to etch with reactive plasma than other common materials in IC technology. If the process parameters are not optimized, their etching rates are even lower than those of mask materials used for etching.⁴ The consequences of low volatility of the etching products are not only low etching rates, but also gradual sidewall slopes of the etched structures and redeposition of etching residues on the etched structures.

In RIE processes, not only the material which is supposed to be etched but also the mask material can be etched by reactive ions on both upper and lateral sides. Mask thickness and lateral dimensions decrease during etching. If the lateral dimension of an etching mask decreases rapidly during etching, the sidewall of etched material will have a gradual slope. In an ideal etching process, the selectivity (etching rate of target material/etching rate of mask) should be high enough to ensure a steep sloped sidewall. In the case of a ferroelectric capacitor, the sidewall slope is usually lower than 75° because of low selectivity.^{5,6} This results in wasted areas at the capacitor edge and makes scale down of ferroelectric capacitors more difficult.

^aE-mail: bodo.kalkofen@ovgu.de

TABLE I. Melting points and boiling points of halides of iridium.¹⁻³

Compound	mp (°C)	bp (°C)
IrF ₃	250 dec	-
IrF ₆	44	53
IrCl ₂	>733 dec	-
IrCl ₃	763 dec	-
IrCl ₄	~700 dec	-

dec: decompose

Because of the low volatility of the etching products, higher DC bias and additional Ar gas are often used in RIE processes to enhance the etching rate by physical ion sputtering. The drawback is redeposition of sputtered nonvolatile etching products and fence formation on the edges of the etching mask and etched material.⁷ A further problem can occur if the whole capacitor stack is etched at one time with a single mask process: redeposition of conductive etching residues from the electrodes onto sidewalls of the ferroelectric material causes leakage currents between top and bottom electrodes.^{8,9}

Because of the low volatility of the etching products, a higher temperature etching process for ferroelectric capacitors is, therefore, necessary in order to enhance the etching rate. This demand results in a new problem: Photoresists are not suitable as etching masks for high temperature etching. SiO₂, TiN, TiAlN, etc. have been studied as etching masks instead of photoresist for high temperature RIE.^{5,9-12} Unfortunately, although the etching rates of ferroelectric and electrode materials are increased in high temperature etching processes, the sidewall slopes of ferroelectric capacitors after etching are still too gradual because of low selectivity between mask materials and ferroelectric/electrode materials. It is therefore necessary to find a new mask material with higher selectivity for iridium etching.

Table II shows the melting points and boiling points of halides of aluminum. It is shown that its fluoride (AlF₃) has a much higher melting point than fluorides of iridium (IrF₃, IrF₆). Hence it may be possible to use Al or Al₂O₃ as etching mask with high selectivity for reactive ion etching of Ir under high temperature with fluorine-containing chemistries such as CF₄, SF₆ or NF₃. Al is already used for metal wires in conventional CMOS process. Al₂O₃ is also used in FeRAM processes as hydrogen barrier layer and is proved to be compatible with conventional CMOS process technology. Using of both Al and Al₂O₃ should cause no problem with CMOS devices and ferroelectric capacitors.

Fluorocarbon plasmas have been investigated since many years. The dissociation of CF₄ in the plasma is a very complicated procedure.¹³⁻¹⁸ In RIE of Si and SiO₂, the dissociated fluorine atoms are responsible for etching. They react with Si and SiO₂ and form volatile SiF₄ which leaves the substrate surface thereafter.

It is well known that the addition of a small amount of O₂ into the CF₄ plasma can enhance the atomic fluorine concentration and therefore enhances the etch rate. The mechanism of dissociation becomes more complicated with the addition of O₂.¹⁸⁻²¹ Earlier studies have reported that the atomic F concentration increases up to a maximum at a certain O₂ percentage. Further increasing of O₂ percentage causes a decrease of the F concentration. This decrease is probably caused by dilution. A strong relation between F concentration and etch rate of Si and SiO₂ was also found.^{13,22,23}

TABLE II. Melting points and boiling points of halides of aluminum.¹⁻³

Compound	mp (°C)	bp (°C)
AlF ₃	1040	1537
AlCl ₃	192.6	180 sub
AlBr ₃	97.5	255

sub: sublime

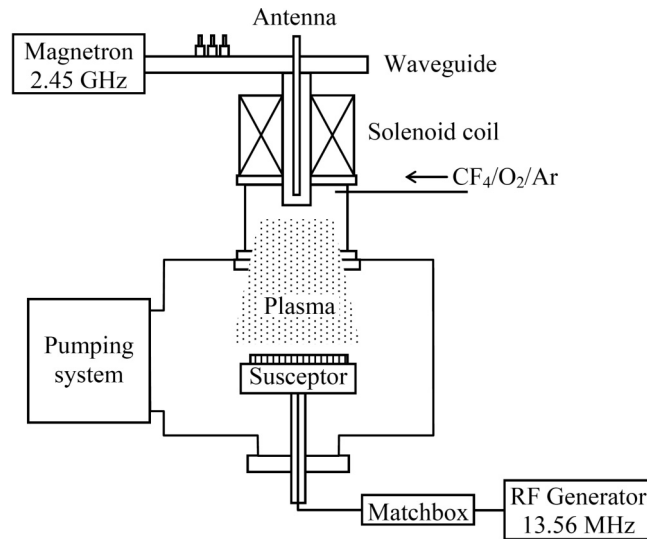


FIG. 1. Schematic diagram of the ECR-RIE system.

It should be noted that in addition to the dissociation and reaction of CF_4 in the plasma, fluorocarbon radicals can form polymers on the substrate surface. The deposited polymer layer inhibits the etching by preventing fluorine atoms to reach the Si or SiO_2 surface. The added O_2 reacts with fluorocarbon radicals in the plasma to form CO and CO_2 and reduces the formation of fluorocarbon polymers. This is another benefit of adding O_2 in CF_4 plasma. Adding argon in the plasma is also an alternative to remove the polymers by Ar ion bombardment.

The knowledge about RIE of Si and SiO_2 with fluorine-containing gases provides a starting point for etching of iridium and aluminum with the same kind of gases. In this study, RIE of iridium thin films under elevated process temperatures was investigated with thin aluminum films as etching mask and $\text{CF}_4/\text{O}_2/\text{Ar}$ as etching gases.

II. EXPERIMENTAL

The experiments were carried out in an electron cyclotron resonance (ECR) enhanced reactive ion etching system which is shown in Figure 1. The ECR plasma was generated by microwave at the upper side of the chamber and introduced into the process chamber. The wafer was located on a resistor heated chuck. A DC bias at -200V was applied to the chuck by an RF generator with a matchbox. This is a moderate bias which is just enough to prevent polymer deposition but leads to only small degree of physical sputtering of iridium so that etching is dominated by the effects of the chemical reactions. The total gas flow was kept at 50sccm . The process conditions are summarized in Table III.

Iridium substrates used for these experiments were prepared on p-type $\langle 100 \rangle$ silicon wafers. The wafers were thermally oxidized to form 500 nm SiO_2 . A thin Ti film of 20 nm thickness was then

TABLE III. Process conditions for iridium etching.

Substrate	Al/Ir/Ti/ SiO_2 /Si Ir/Ti/ SiO_2 /Si
Substrate temperature	$25\text{--}350^\circ\text{C}$
Process pressure	$0.006\text{--}0.013\text{mbar}$
Co-reactant gases	$\text{CF}_4/\text{O}_2/\text{Ar}$
ECR microwave power	$200\text{--}600\text{W}$
RF DC bias	-200V
RF power (variable to fit DC bias)	$20\text{--}70\text{W}$

deposited by e-beam evaporation onto SiO₂ and was used to improve the adhesion of the following iridium film. An iridium film of 150 nm thickness was then deposited also by e-beam evaporation onto the Ti film. Because of limitations of process issues in our laboratory, the lift-off method, instead of dry/wet Al etching, was used to form Al patterns on iridium for use as etching mask. Photoresist was patterned on the Ir-covered wafers according to process parameters of the lift-off method. After performing this lithography process, a 100 nm thick Al film was deposited on the wafers by e-beam evaporation. The wafers were afterwards immersed in acetone to remove photoresist and also the aluminum deposited on the photoresist. The aluminum which was deposited directly on the iridium surface was not removed and stayed on the iridium as etching mask. An O₂ plasma treatment at 300 °C for one hour was performed to remove the possible residue of photoresist on the surfaces of Ir and Al films. Wafers with 100 nm Ir films but without Al etching mask were also used in the experiments for estimations of the Ir etching rate.

The etch rate was calculated with help of step height measurements by a Dektak Profilometer on the edge of Al mask patterns. The Al mask patterns for measurement are 10/10 μm line/space structures. The Al mask thickness d_1 was measured at first before etching. The samples were then etched in the chamber for t minutes using various process conditions. After etching the samples were measured with the Profilometer for the second time and the step height determined was d_2 . The Al etching mask on iridium was then removed by a wet etching process with commercial Al etch solution (73.1% H₃PO₄ + 2.3% HNO₃ + 22.3% CH₃COOH) at room temperature without damaging the Ir surface because Ir is not attacked by any acid solution including aqua regia. After Al removal, the samples were measured by Profilometer for the third time and the step height d_3 was obtained. The etch rates of Ir and Al were then calculated as follows:

$$\text{Ir etch rate} = d_3/t$$

$$\text{Al etch rate} = (d_1 + d_3 - d_2)/t$$

$$\text{Selectivity} = \text{Ir etch rate} / \text{Al etch rate}$$

In the experiments the influence of various process parameters such as gas mixing ratio and substrate temperature on the etch rate was investigated. The samples after etching were inspected under SEM to evaluate the surface profile.

III. RESULTS AND DISCUSSION

A. CF₄/O₂/Ar gas mixing ratio

The influence of the CF₄/O₂/Ar gas mixing ratio on the etch rate is shown in Figure 2. The samples were etched at 300 °C and 0.01 mbar with 400W ECR power and the total gas flow was kept at

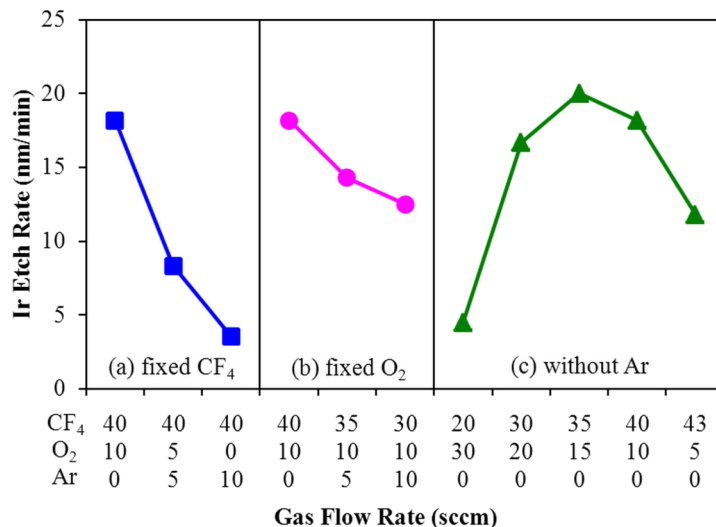


FIG. 2. Effect of gas flow rates on etch rate of Ir in CF₄/O₂/Ar plasmas.

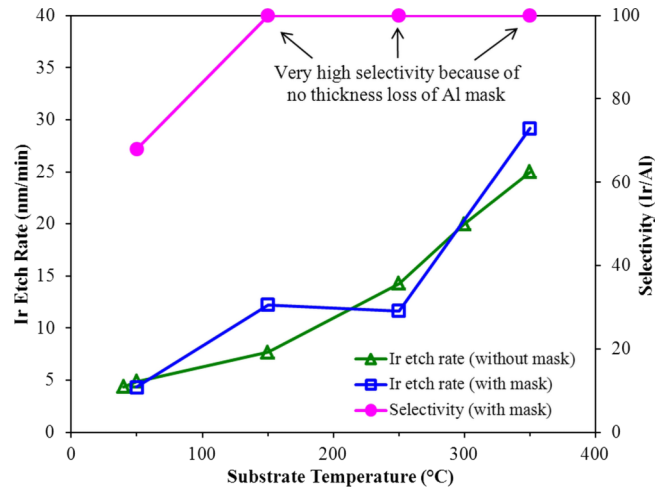


FIG. 3. Effect of substrate temperature on etch rate of Ir in CF_4/O_2 plasmas.

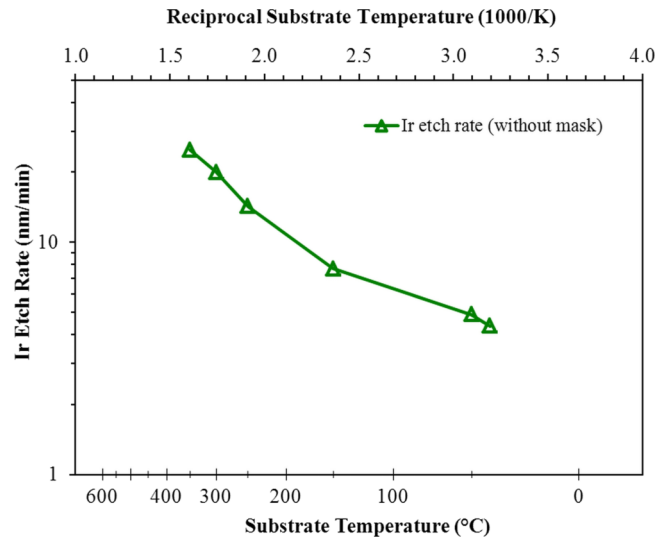


FIG. 4. Arrhenius plot of the etch rate of Ir in CF_4/O_2 plasmas.

50 sccm. In Figure 2(a) the CF_4 flow rate was fixed at 40 sccm and only O_2 and Ar flow rates were changed. The etch rate decreases when O_2 is replaced by Ar. Although both Ar and O_2 can reduce polymer deposition, the result shows that O_2 works better than Ar with respect to enhancing the etch rate. The reason may be the role of O_2 in enhancing the dissociation of CF_4 which results in higher concentration of fluorine radicals.

In Figure 2(b) the flow rate of O_2 was fixed at 10 sccm and CF_4/Ar flow rates are changed. Increasing the Ar flow rate and decreasing the CF_4 flow rate causes a decrease of the etch rate. It seems that the gain in etch rate by reducing polymer film growth with Ar ion bombardment is smaller than the loss of etch rate caused by replacing an equal amount CF_4 by Ar. The results of Figure 2(a) and 2(b) indicate that the addition of Ar in the CF_4/O_2 gas mixture may be profitless for Ir etching.

The gas mixing ratio of CF_4/O_2 without Ar was investigated and the result is shown in Figure 2(c). Adding of O_2 up to 30% ($\text{CF}_4=35$ sccm, $\text{O}_2=15$ sccm) results in the highest etch rate. A further increase of O_2 beyond 30% causes a decrease of the etch rate. This phenomenon is similar to the results found in earlier studies of Si/SiO₂ etching with CF_4/O_2 plasmas.^{13,24,25}

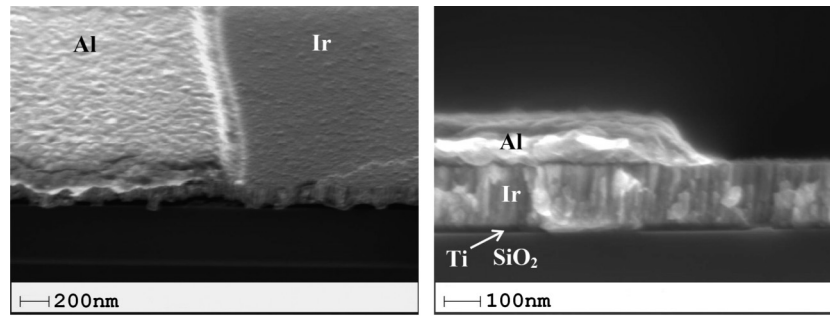


FIG. 5. SEM images of the Ir films and Al masks before etching.

B. Substrate temperature

The effect of substrate temperature on etch rate and selectivity is shown in Figure 3. The etch rate of Ir increases in general with increasing temperature. The etch rate is higher than about 25 nm/min at 350 °C and is about five times higher than the etch rate at room temperature. The selectivity (Ir/Al) at room temperature is nearly 70. The thickness loss of the Al mask after etching is usually only in the range of one nanometer; sometimes the Al mask is even a few nanometers thicker than before etching. But these thickness changes are smaller than the measurement uncertainty. Therefore the etch rate of the Al mask is negligible and, in comparison to the etch rate of Ir, the selectivity is very high. Good etching profiles at sidewalls of Ir should be achievable as long as the sidewall profile of the Al mask is good enough.

Figure 4 shows an Arrhenius plot of the Ir etch rate in CF_4/O_2 plasmas. The temperature dependence of the etch rate seems to be non-Arrhenius. The whole etching reaction consists of several mechanisms including absorption of reactants on the surface, surface reaction, inhibition caused by polymer deposition, ion-enhanced reaction, desorption of low volatile products from the surface,

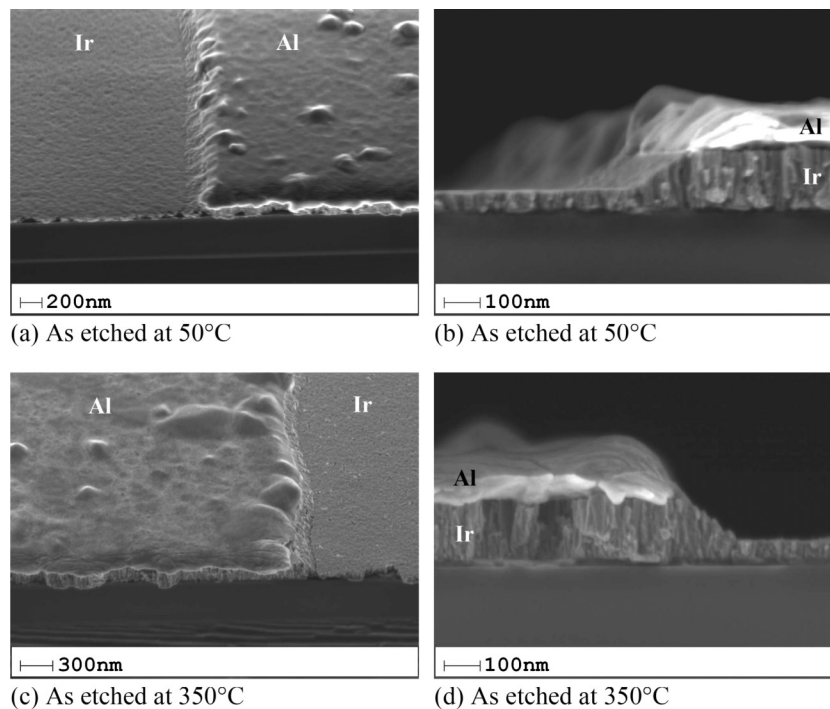


FIG. 6. SEM images of the Ir films and Al masks after etching.

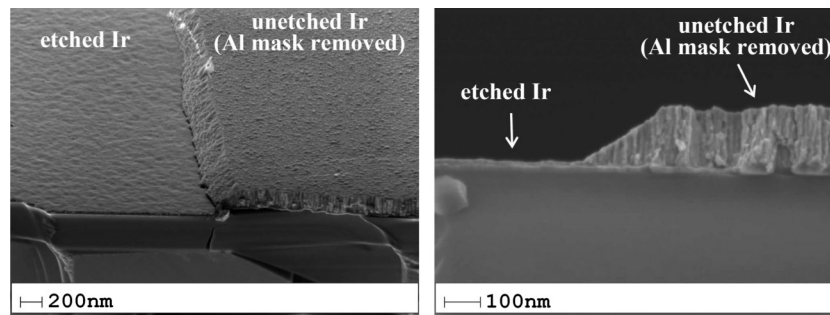


FIG. 7. SEM images of the Ir films etched at 100°C after Al mask removal.

ion-assisted products/polymer removal from the surface, etc. In addition to the surface reaction rate, it is known that deposition of fluorocarbon polymer and desorption of low volatile products play also important roles for the etch rate in such a system. Due to the influence of so many factors, it seems plausible that the etch rate cannot be characterized by an Arrhenius equation with a single activation energy.

C. Surface profile

The samples were inspected with SEM after the experiments. A bird's view and a cross-sectional view of the Ir film and the Al mask before etching are shown in Figure 5. Unfortunately, the sidewall of the Al mask pattern made by the lift-off method is not vertical but shows a very gradual slope. A vertically etched sidewall is usually not possible with such an etching mask.

The samples etched at 50 °C and 350 °C are shown in Figure 6. Both the Ir surface and the Al surface are clean after etching. No fences or residues on the sidewalls are visible. In addition, although Al is supposed to form nonvolatile products with F, the etched Ir surface is smooth without micromasking effect. The slope of the etched Ir sidewalls is around 45°. It is found that many hillocks form on the Al mask after etching. The reason is still unknown. As the hillock formation occurs at low and high temperatures, the etching temperature should not be the key issue.

The Ir film etched at 100 °C after Al mask removal is shown in Figure 7. The whole surface, including the etched Ir area, the etched Ir sidewall and the unetched Ir area under the Al mask, is clean without any residue. The unetched Ir area under the Al mask is still smooth after etching and Al mask removal. That means the location of hillocks shown in Figure 6 should be above the Ir film and the hillocks cannot stem from the Ir film under the Al mask.

IV. CONCLUSION

Reactive ion etching technology for iridium was developed in this study. $\text{CF}_4/\text{O}_2/\text{Ar}$ gas mixtures were used with an aluminum film as hard mask for Ir etching at high temperatures. According to the results, the addition of Ar to the gas mixture seems to be profitless. The optimum gas mixing ratio is $\text{CF}_4/\text{O}_2 = 35 \text{ sccm}/15 \text{ sccm}$. The high process temperature at 350 °C enhances the Ir etch rate to about 25 nm/min, which is about five times higher than the etch rate at 50 °C. All investigated processes at temperatures ranging from room temperature up to 350 °C exhibit very high etching selectivities. Neither visible residues on the etched surfaces nor fences at the etched sidewalls could be detected. The surfaces of Ir are clean and smooth after etching independent on the etching temperature. Nevertheless, many hillocks form on the Al mask after etching and the reason for it is still unknown. The results show that aluminum is a suitable mask material for iridium etching with CF_4/O_2 plasma at high process temperatures. This technology can be applied to industrial production of FeRAM with Ir electrodes.

¹ David R. Lide, *CRC Handbook of Chemistry and Physics*, 84th ed. (CRC Press, 2003).

² Carl L. Yaws, *Chemical properties handbook* (McGraw-Hill, 1999).

³ <http://www.webelements.com>.

- ⁴ Se-Geun Park, Chin-Woo Kim, Ho-Young Song, Hyoun Woo Kim, Ju Hyun Myung, Sukho Joo, Soon Oh Park, and Kyu-Mann Lee, *J. Mater. Sci.* **40**(18), 5015 (2005).
- ⁵ Francis G. Celii, Mahesh Thakre, Mark K. Gay, Scott R. Summerfelt, Sanjeev Aggarwal, J. Scott Martin, Lindsey Hall, K. R. Udayakumar, and Ted S. Moise, *Integr. Ferroelectr.* **53**, 269 (2003).
- ⁶ D. J. Jung, W. S. Ahn, Y. K. Hong, H. H. Kim, Y. M. Kang, J. Y. Kang, E. S. Lee, H. K. Ko, S. Y. Kim, W. W. Jung, J. H. Kim, S. K. Kang, J. Y. Jung, H. S. Kim, D. Y. Choi, S. Y. Lee, K. H. A , C. Wei, and H. S. Jeong, *IEEE Symp. VLSI Technol., Dig. Tech. Pap.* **102** (2008).
- ⁷ F. G. Celii, T. S. Moise, S. R. Summerfelt, L. Archer, P. Chen, S. Gilbert, R. Beavers, S. M. Bilodeau, D. J. Vestyck, S. T. Johnston, M. W. Russell, and P. C. Van Buskirk, *Integr. Ferroelectr.* **27**, 227 (1999).
- ⁸ J. H. Park, H. H. Kim, N. W. Jang, Y. J. Song, H. J. Joo, H. Y. Kang, S. Y. Lee, and Kinam Kim, *Integr. Ferroelectr.* **53**, 307 (2003).
- ⁹ Ulrich Egger, Kazuhiro Tomioka, George Stojakovic, Yasuyuku Taniguchi, Rainer Bruchhaus, Haoren Zhuang, Hiroyuki Kanaya, Gerhard Beitel, and Shigeki Sugimoto, *Mat. Res. Soc. Symp. Proc.* **748**, U1.7.1 (2003).
- ¹⁰ K. L. Saenger, P. C. Andricacos, S. D. Athavale, J. D. Baniecki, C. Cabral, Jr., G. Costrini, K. T. Kwietniak, R. B. Laibowitz, J. J. Lian, Y. Limb, D. A. Neumayer, and M. L. Wise, *Mat. Res. Soc. Symp. Proc.* **655**, CC2.1.1 (2000).
- ¹¹ Jer-shen Maa, Hong Ying, and Fengyan Zhang, *J. Vac. Sci. Technol. A* **19**(4), 1312 (2001).
- ¹² Chris Ying, Reggie Mananquil, Ryan Patz, Amitabh Sabharwal, Ajay Kumar, Francis Celii, Mahesh Thakre, Mark Gay, Robert Kraft, Scott Summerfelt, and Ted Moise, *Integr. Ferroelectr.* **53**, 325 (2003).
- ¹³ C. J. Mogab, A. C. Adams, and D. L. Flamm, *J. Appl. Phys.* **49**, 3796 (1978).
- ¹⁴ Koji Miyata, Hori Masaru, and Goto Toshio, *J. Vac. Sci. Technol. A* **14**(4), 2343 (1996).
- ¹⁵ Da Zhang and Mark J. Kushner, *J. Vac. Sci. Technol. A* **18**(6), 2661 (2000).
- ¹⁶ T. Kimura and K. Ohe, *J. Appl. Phys.* **92**, 1780 (2002).
- ¹⁷ Jung-Hyung Kim, Kwang-Hwa Chung, and Yong-Shim Yoo, *J. Korean Phys. Soc.* **47**(2), 249 (2005).
- ¹⁸ Tomoyuki Kuroki, Junko Mine, Masaaki Okubo, Toshiaki Yamamoto, and Noboru Saeki, *IEEE Trans. Ind. Appl.* **41**(1), 215 (2005).
- ¹⁹ M. Dalvie and K. F. Jensen, *J. Vac. Sci. Technol. A* **8**(3), 1648 (1990).
- ²⁰ Glauco F. Bauerfeldt and Graciela Arbilla, *J. Braz. Chem. Soc.* **11**(2), 121 (2000).
- ²¹ H. D. Xie, B. Sun, X. M. Zhu, and Y. J. Liu, *Int. J. Plasma Environ. Sci. Technol.* **3**(1), 39 (2009).
- ²² Daniel L. Flamm and Vincent M. Donnelly, *Plasma Chem. Plasma Process.* **1**(4), 317 (1981).
- ²³ R. d'Agostino, P. Capezzuto, G. Bruno, and F. Cramarossa, *Pure & Appl. Chem.* **57**(9), 1287 (1985).
- ²⁴ Akiyoshi Nagata, Hideki Ichihashi, Yasutomo Kusunoki, and Yasuhiro Horiike, *Jpn. J. Appl. Phys.* **28**, 2368 (1989).
- ²⁵ B. E. E. Kastenmeier, P. J. Matsuo, J. J. Beulens, and G. S. Oehrlein, *J. Vac. Sci. Technol. A* **14**(5), 2802 (1996).